THE ASTROPHYSICAL JOURNAL, 365:487–501, 1990 December 20

EXTENDED Lyα EMISSION ASSOCIATED WITH 3C 294[1]

PATRICK J. MCCARTHY,[2,3,4] HYRON SPINRAD,[2,5,6] WIL VAN BREUGEL,[2,4] JAMES LIEBERT,[7]
MARK DICKINSON,[2,5,6] S. DJORGOVSKI,[5,8] AND PETER EISENHARDT[2,5,9]
Received 1989 April 20; accepted 1990 June 15

ABSTRACT

We report the discovery of a large cloud of ionized gas associated with the radio galaxy 3C 294 at a redshift of 1.786. The radio source is a powerful double with a weak core. We detect Lyα emission with a total monochromatic luminosity of $L_{\mathrm{Ly}\alpha} = 7.6 \times 10^{44}$ ergs s^{-1} extended over $\sim 100 \times 170$ kpc. The emission-line cloud is highly elongated and is well aligned with the inner radio source axis. Long-slit spectra, taken along the major axis, show spatially extended emission lines of N V λ1240, C IV λ1550, He II λ1640, and C III λ1909. The extended Lyα emission shows a large, smooth velocity gradient (1500 km s^{-1}) and large intrinsic line widths (700–2600 km s^{-1}). The high-ionization lines, particularly C IV, show large velocity changes that are systematically different from those of Lyα.

3C 294 appears to be another, even more spectacular member of a class of powerful radio galaxies at high redshift typified by 3C 326.1. We discuss our observations from the point of view of star formation and the interaction of nuclear activity with ambient material. We consider two scenarios for the ionization of the Lyα cloud: ionization by a population of extremely massive stars and ionization by a nonthermal continuum from the radio nucleus. Stellar photoionization appears to be insufficient in both the total number of ionizing photons and its ability to produce highly ionized species. We propose that the 150 kpc cloud of gas is photoionized by a central nonstellar source. We detect a very red compact object at 2.2 μm nearly coincident with the radio core. It is unclear whether the light from this object is primarily stellar or nonstellar.

Subject headings: galaxies: evolution — galaxies: individual (3C 294) — galaxies: redshifts — radio sources: galaxies

I. INTRODUCTION

Early radio observations of 3C 294 with the Cambridge 5 km telescope were reported by Jenkins, Pooley, and Riley (1977). These observations showed it to be a strong (S_{178} = 10.3 Jy) source with extended structure. Optically, the source remained unidentified until the present work, in large part because of the presence of a $V = 12$ mag subgiant K star, only 10″ to the west of the radio centroid (Kristian, Sandage, and Katem 1974; Riley, Longair, and Gunn 1980). Current ground-based imaging with any detector is hampered by scattered light from this Galactic star.

Given that many of the recently identified 3CR sources are associated with faint galaxies having strong Lyα emission (Spinrad *et al.* 1985), and in some cases *very extended* Lyα emission (McCarthy *et al.* 1987*a*), it seemed reasonable that 3C 294 might be detectable spectroscopically, without the benefit of an optical identification. After receiving a report of a tentative radio core detection by R. A. Laing and F. N. Owen (1986, private communication), we planned a "blind" spectroscopic observation of this location in hopes of detecting strong Lyα emission. Such an observation was carried out by one of us (J. L.) on 1987 January 27 UT with the Multiple Mirror Telescope and its intensified Reticon spectrograph (Latham 1982). The spectrograph aperture was offset from the K star to the radio position. A 3600 s observation led to the detection of a strong emission line at 3390 Å. This emission line was interpreted to be Lyα at a redshift of 1.786. Subsequent observations, described below, have confirmed this. A similar observation, this time with a long slit, was performed at Lick Observatory on 1987 May 1 UT. This observation, made under very poor conditions, confirmed the emission line at 3390 Å, and, most important, showed the emission to be very extended (>7″) along the slit.

These initial observations were followed up with detailed observations at a number of observatories which together reveal a most unusual object. The enormous Lyα emission-line cloud associated with 3C 294 is, in many ways, similar to that associated with 3C 326.1 (McCarthy *et al.* 1987*a*) and other distant radio galaxies, but is much richer in its spatial and kinematic properties. These objects, with their extremely faint optical continua, have no known low-redshift counterparts and may be revealing to us the late stages of galaxy formation. The strong radio/optical correlations in this and similar high-redshift radio galaxies suggest that we are witnessing the early development of powerful radio sources in dense gaseous environments.

We discuss our optical, radio, and infrared observations in § II, give possible interpretations of our results in § III, and provide a summary in § IV. A complete journal of our observations is presented in Table 1.

[1] Based, in part, on observations obtained at Lick Observatory, which is owned and operated by the University of California, and the Multiple Mirror Observatory, a joint facility of the Smithsonian Astrophysical Observatory and the University of Arizona.

[2] University of California, Berkeley.
[3] The Observatories of the Carnegie Institution of Washington.
[4] Guest Investigator, Very Large Array. The VLA is a facility of the National Radio Astronomy Observatory, which is operated by Associated Universities, Inc., under contract with the National Science Foundation.
[5] Guest Investigator, Kitt Peak National Observatory, National Optical Astronomy Observatories, which is operated by Associated Universities for Research in Astronomy, Inc., under contract with the National Science Foundation.
[6] Guest Investigator, Multiple Mirror Telescope.
[7] Steward Observatory, University of Arizona.
[8] Division of Mathematics, Physics, and Astronomy, California Institute of Technology.
[9] NASA–Ames Research Center.

TABLE 1

JOURNAL OF OBSERVATIONS

A. OPTICAL IMAGING

Date 1987	Telescope	Filter (Å)	Integration (s)	Observers	Comments
Jun 20.....	KPNO 4 m	3380/50	4800	H. S., M. D.	Lyα
Jun 21.....	KPNO 4 m	3380/50	3200	H. S., M. D.	Lyα
Jun 22.....	KPNO 4 m	3500/50	3520	H. S., M. D.	"Off-band"

B. RADIO IMAGING (VLA)

Date 1987	Array	Frequency	Integration (s)	Observers	Comments
Jun	A	4985 MHz	1800	W. vB., P. M.	0".4 resolution

C. INFRARED IMAGING

Date 1989	Telescope	Filter	Integration (s)	Observers	Comments
Apr 16.....	KPNO 4 m	K (2.16 μm)	3600	P. E., M. D.	60 × 60 s
Apr 19.....	KPNO 4 m	J (1.24 μm)	1920	P. E., M. D.	8 × 240 s

D. APERTURE SPECTROSCOPY (MMT)

Date 1987	Resolution (Å)	Offset $\Delta\alpha$, $\Delta\delta$ (arcsec)	Integration (s)	Observers	Comments
Jan 27.....	12	9, −1.5	3600	J. L.	Discovery spectrum
Mar 30.....	12	9, −1.5	3600	J. L.	Lyα only
Apr 25.....	12	9, −1.5	3600	J. Huchra	Lyα blue wing
Jun 27.....	12	10, +1	4800	M. D.	Lyα, C IV, He II, N V

E. SLIT SPECTRA (LICK)

Date 1987	Offset (arcsec)	P.A.	Integration (s)	Observers	Comment
May 1.....	10, −1	180°	3600	H. S., P. M.	Discovery spectrogram
May 2.....	0, 0	270	3600	H. S., P. M.	Poor seeing
Jul 1.....	10, 0	190	4000	P. M., M. D.	Lyα, C IV, He II, C III], N V
Jul 2.....	9, −1	210	4000	P. M., M. D.	Lyα
Jul 3.....	10, 0	190	4000	P. M., M. D.	Lyα, C IV, He II, C III], N V
Jul 27.....	9, 0	190	4000	H. S., M. D.	Lyα

II. OBSERVATIONS AND REDUCTIONS

a) Optical Imaging

To follow up the discovery observations described above, we began with interference filter imaging in the light of Lyα. The observations were made to investigate the spatial morphology of the gas and to plan for further detailed spectroscopy.

Direct-imaging observations were made in 1987 June with the Kitt Peak Mayall 4 m telescope, its prime-focus camera, and RCA No. 1 CCD. For these observations we acquired interference filters optimized for 3C 294. These consisted of an "on-band" filter for redshifted Lyα with $\lambda_0 = 3380$ Å, $\Delta\lambda = 50$ Å and an "off-band" filter with $\lambda_0 = 3500$ Å, $\Delta\lambda = 50$ Å for an attempt at observing the galaxy's continuum. The imaging detector was a thinned RCA CCD used in 32 row short-scan mode to average over pixel-to-pixel variations within columns. Three exposures, each 3200 s long, were made with the "on-band" filter on 1987 June 20 and 21 UT. Photometric transparency was good, and the seeing FWHM was ~1".5 on both nights. On 1987 June 22 UT a 2560 s exposure was taken using the off-band filter under similarly good conditions. Short exposures of the photometric standard star HZ 44 (Oke 1974) were taken each night through the same filters in order to allow flux calibration. The data were reduced using standard techniques.

The Lyα images were shifted into mutual registration using two stars in the field to determine the relative offsets. The data were then co-added to produce a single frame with 9600 s of integration. The center of the K star next to 3C 294 was slightly saturated in the images, and a low-level bleed trail projects to the west, away from the radio galaxy. Scattered starlight from the star remained a significant contributor to the background brightness at the position of the galaxy. This was removed by subtracting a model of the star from the actual image. First, the radial brightness profile of the star was determined using circular apertures, with both 3C 294 and the bleed trail to the west excluded from the areas measured. This profile was smoothed slightly, and a circularly symmetric model star was generated to match it. Finally, the model was shifted into

registration with the actual K star and subtracted from the image. The saturated center of the star is poorly removed by this approach, but the scattered light in the wings beyond a 3″ radius is essentially eliminated.

Our "off-band" imaging observations failed to detect the continuum from the galaxy, our upper limit for any unresolved knots being $m_{AB3500} > 20.2$ mag, where $m_{AB} \equiv -48.60 - 2.5 \log f_\nu$ (cgs). Assuming $H_0 = 50$ km s^{-1} Mpc^{-1} and $q_0 = 0$, as we do throughout this paper, this corresponds to $M_{AB1400} > -25.2$ at the redshift of 3C 294. We have detected the optical continuum at a fainter level spectroscopically (see § II*e*) and in infrared images (§ II*c*).

We will use the K star as our positional reference point. Astrometric positions for this star are given in Véron (1966), Kristian, Sandage, and Katem (1974), and Riley, Longair, and Gunn (1980). Unfortunately, the agreement of these three independent positions is only fair, with the uncertainties being $\Delta\delta = 0\farcs6$ and $\Delta\alpha = 0\farcs3$. We have adopted a mean position for the K star of

$$\alpha(1950) = 14^h04^m33^s.24, \quad \delta(1950) = 34°25'38\farcs9 .$$

In describing the various observations and results, we will specify positions by the last arguments of their right ascension and declination, denoted by α^*, δ^*. In this notation the K star is at $\alpha^* = 33^s.24$, $\delta^* = 38\farcs9$.

A contour representation of our co-added image is shown in Figure 1*a*. Superposed on the contours are the positions of features in the radio maps. Figure 1*a* illustrates the large size and elongated shape of the cloud. From this contour map we determine a maximum size of 15″ and an axial ratio of 1.7:1 at an observed surface brightness level of 10^{-16} ergs s^{-1} cm^{-2} arcsec^{-2}. The long axis of the emission cloud is oriented nearly north-south, in position angle 178°. The highest surface brightness region is 2″ north of the radio core (see below). From our images we determined a spatially integrated Lyα line flux of 1.55×10^{-14} ergs s^{-1} cm^{-2}. This translates to a monochromatic luminosity of 7.6×10^{44} ergs s^{-1}.

b) Radio Imaging

Multifrequency observations of 3C 294 were made with the Very Large Array in the A- and B-arrays (Thompson *et al.* 1980) in 1987 September and in 1987 December. A total of 10 frequency settings were used, and a detailed discussion of all these observations will be given elsewhere. Here we present the 6 cm A-array data, which, at a resolution of 0″.4, show the most detail.

Our 6 cm total intensity map is shown in Figure 2. The source consists of five more or less distinct structures. These are a central component (C), the northern and southern knots, the northern and southern hot spots, and the lobe or jetlike feature to the southwest. Gaussian model fits show that the central component C is unresolved (< 0″.31), and that the knots are slightly extended in the directions of their associated hot spots. Component C has a flux density of 0.56 ± 0.07 mJy at 4985 MHz, and was not detected at a level of 0.63 mJy (3 σ) at 1465 MHz. Thus it has a flat or inverted spectrum. Its position is $\alpha^* = 34^s.060 \pm 0^s.005$, $\delta^* = 40\farcs00 \pm 0\farcs05$. Based on its compactness, flat/inverted spectrum, and central location, we believe that component C is the core of the radio source and is to be identified with the active nucleus of 3C 294. The previously suggested identification by Laing and Owen is actually the southern knot.

The overall morphology of the source is slightly Z-shaped. This morphology can be most easily interpreted as the result of a precessing or torqued jet. While it is possible that the sharp bends in the source structure at the two knots may be caused by sudden changes in the ambient pressure (they occur at the edges of the Lyα cloud), the overall Z-shaped symmetry of the source argues strongly for a sudden change in the direction of outflow from the nucleus, or shearing of the radio source by

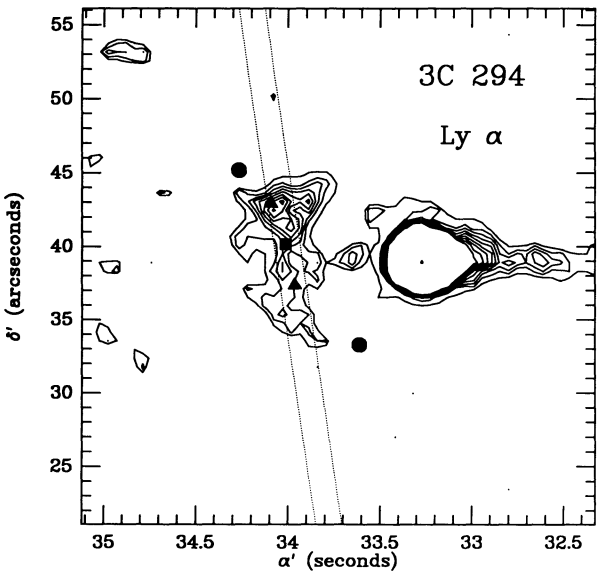

FIG. 1*a*

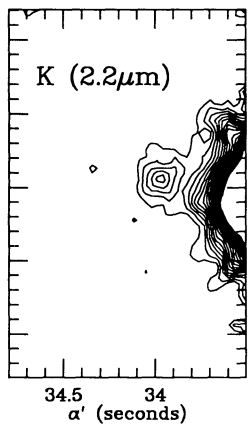

FIG. 1*b*

FIG. 1.—(*a*) Lyα interference filter image of 3C 294. The contours, in units of 10^{-16} ergs s^{-1} cm^{-2} arcsec^{-2}, are 1.3, 2.0, 2.8, 3.6, 4.4, 5.2, and 6.0. The residual image of the K star (after subtraction of a model) is clearly visible at $\alpha^* = 33^s.24$, $\delta^* = 38\farcs9$; a CCD bleed trail extends west from the star. The positions of the radio core (*square*), radio knots (*triangles*), and radio lobes (*filled circles*) are schematically marked. The orientation of the spectrograph slit for the 1988 July 1 and 3 observations is shown by the dotted line. (*b*) Contour representation of our *K*-band image of 3C 294, on the same scale as the Lyα image in (*a*). Contour levels (in μJy arcsec^{-2}) are 4.3, 6.4, 8.5, 10.7, 12.8, 14.9, 17.0.

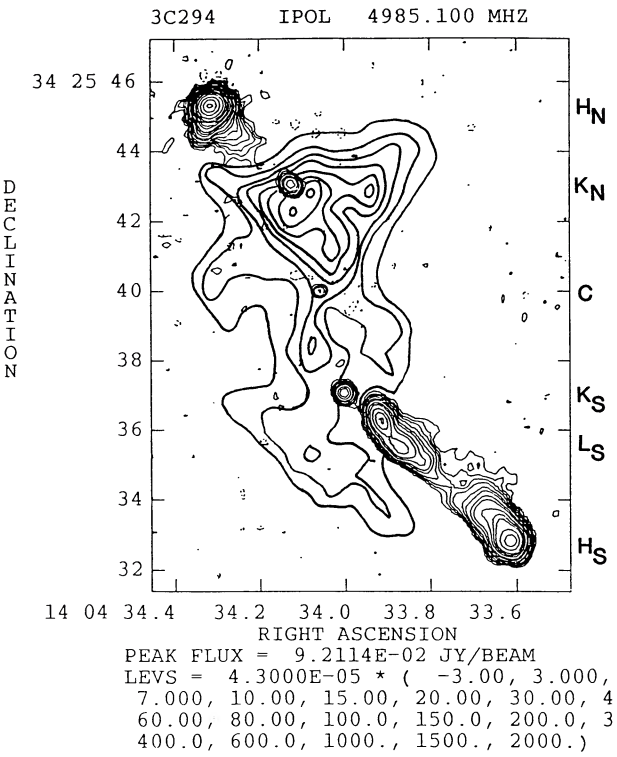

FIG. 2.—Shown are the 6 cm total intensity of 3C 294 (*thin contours*), with the Lyα image superposed (*dashed contours*). Various radio features discussed in the text are marked: C (core), K_N and K_S (knots), H_N and H_S (hot spots) and L_S (lobe or jet). Note the bright line emission near knot K_N, and the slight misalignment between the radio axis and the emission-line cloud.

rotation of the ambient medium (note that lines connecting the knots to their nearest hot spots are parallel).

The radio core is symmetrically located between the two knots which have comparable surface brightnesses and total flux densities, but the hot spots are very asymmetric. The arm length ratio, defined as the ratio of the largest core/hot spot distance (to the south) to the smallest core/hot spot distance (to the north), is 1.48. The flux density ratio of the brightest (to the north) and faintest (to the south) lobes/hot spots in 3C 294 is 2.36, and the corresponding surface brightness ratio is 10.7 (at 0".4 resolution). We note that the closer, and brightest, hot spot (north) lies on the side of the higher surface brightness Lyα emission. A correlation between the location of the close hot spot and the higher surface brightness emission-line gas holds for virtually all of the moderate- to high-redshift 3CR radio galaxies (McCarthy, van Breugel, and Kapahi 1990).

c) *Infrared Imaging*

K (2.16 μm) and *J* (1.24 μm) band imaging of 3C 294 was undertaken at Kitt Peak National Observatory under photometric conditions on 1989 April 16 and 19 UT, respectively. The infrared array imager (IRIM; Probst 1988) was employed at the f/8 Cassegrain focus of the 4 m Mayall reflector. The detector is a 58 × 62 pixel InSb array with 76 μm pixels and a scale (in the configuration used) of 0".39 pixel^{-1}. The *K*-band observations were obtained as follows: short exposures of the nearby star (star D) were taken for positional reference. The telescope was then offset in order to move the star off the edge of the detector field of view to avoid saturating the array. Sixty individual frames, each 60 s long, were taken at the object position, with the telescope position displaced by a few arcseconds after every fourth frame using the offset guider. This permitted a median sky flat field to be constructed from the object frames themselves. Short exposures on star D were again taken at the end of the observing sequence to check positioning. The *J* observing sequence was similar, except that eight 240 s frames were taken with offsets after each one.

The individual frames were corrected for dark-current and pixel-response variations, and bad pixels were interpolated over. Modal sky values were then subtracted, and the processed frames were coregistered and combined. Although exposure time (and hence signal-to-noise ratio [S/N]) in the resulting mosaic is a function of position, the region local to the object received a full 3600 s of integration at *K* and 1920 s at *J*. Photometry was calibrated using short exposures of standard stars HD 105601 and HD 136754 for *K* and BD +2°2957 for *J* (Elias *et al.* 1982).

Figure 1*b* shows a contour representation of our *K*-band image. 3C 294 is well detected as a compact object located at $\alpha^* = 33^s.97$, $\delta^* = 40''.5$. This position is 1".3 from the radio core position, but given the uncertainties in the absolute position of the reference star (D) and the radio to optical grid, we do not consider this positional discrepancy significant. Photometry on the frame measures $K = 18.0 \pm 0.3$ within a 3" diameter synthetic aperture.

We are unable to state definitively whether or not the object is extended at *K*. The measured FWHM of star D was 0".85 at *K* in the short (effectively 8 s) frames taken immediately before the integration sequence. This excellent seeing helped by greatly reducing the scattered light from star D, but resulted in our images being slightly undersampled. The formal FWHM for the object is 1".5, but this may be due in part to lower S/N, the undersampling, the long exposure time and multiple shifts, and/or residual scattered light from star D. We measure a FWHM of 1".3 for a faint (but brighter than 3C 294) object known to be a star in a field observed for 2 hours later in the same night with the same techniques. Based on the contour map (see Fig. 1*b*) and visual inspection of the image on a video display device, it is our impression that the object is extended.

The scattered light and seeing were somewhat worse in the *J* image (0".95 FWHM for star D), which prevented us from detecting the object without further processing. We flipped the *J* image about an east-west line centered on star D and subtracted this image from the original. This successfully removed the scattered light from star D near the object, which could now faintly be seen at the same location as in the *K* image. The 3" aperture *J*-magnitude is 21.0, with an estimated uncertainty of 0.4 mag.

d) *Aperture Spectroscopy*

Several aperture spectra were obtained with the Multiple Mirror Telescope, using the MMT spectrograph with an intensified Reticon detector. The initial observation was made with the MMT on 1987 January 27 UT. Several observations using dual apertures, one for sky and one for object plus sky, were made and combined to yield a total of 3600 s of integration. The 3" × 2" aperture was oriented north-south for this and all of the subsequent MMT observations. The aperture was centered at $\alpha^* = 34^s.00$, $\delta^* = 37''.0$. Observations of the K star were made and were used to remove the scattered light from the data. Subsequent observations were made in 1987 March and June.

The observations obtained in 1987 March were centered on

the position reported by Laing and Owen (the southern radio knot), since they were performed prior to our Kitt Peak Lyα imaging observations. These observations showed a strong asymmetry in the Lyα line profile. The asymmetry consists of a blueward wing with a zero-intensity amplitude of 2500 km s^{-1}. These spectra do not show any emission lines other than Lyα. This is consistent with the results of our long-slit spectroscopy as described below.

The MMT observations made in 1987 June were centered on the region of highest Lyα surface brightness, as deduced from our Lyα images. The aperture was centered at $\alpha^* = 34^s.15$, $\delta^* = 42''.0$. Several integrations totaling 4800 s were made in this position. These spectra show strong emission lines of C IV λ1550, He II λ1640, and weak N V λ1240 in addition to Lyα. Our best spectrum from the central regions is shown in Figure 3.

e) *Long-Slit Spectroscopy*

The final, and perhaps most informative, observations were a series of long-slit spectra taken at Lick Observatory in 1987 May and July. These spectra were taken with the Shane 3 m telescope and the Cassegrain grating spectrograph (Miller and Stone 1988). All of the long-slit spectra were taken with a 300 line mm^{-1} grating blazed at 4000 Å. The detector was a UV-sensitized Texas Instruments 800 × 800 CCD. The grating employed gave a pixel size of 4 Å and a wavelength coverage of 3000–6100 Å, with an instrumental resolution that varied (due to focus variations) from 12 to 15 Å. The slit used was $1''.5 \times 2''$, and the spatial size of the pixels was $0''.67$. The slit was aligned in position angles ranging from 180° to 210° (see Table 1). Observations of standard stars from Stone (1977) were used to flux-calibrate the data, and observations of He-Hg-Cd lamps were made after each observation for wavelength calibration.

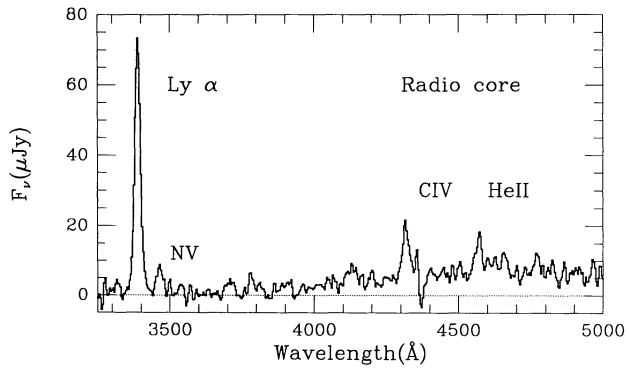

FIG. 3*a*

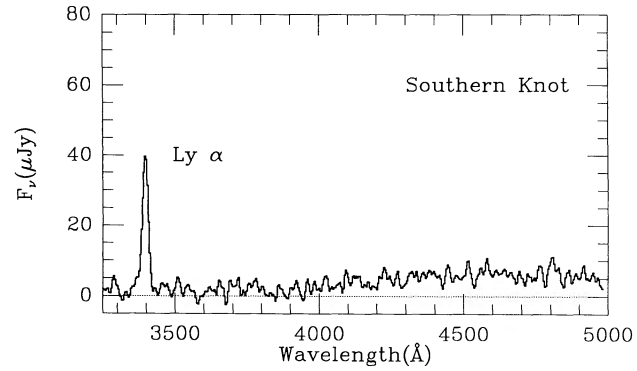

FIG. 3*b*

FIG. 3.—One-dimensional spectra of the core region and the region of the southern radio knot. The scattered light from the K star has been removed, as described in the text. (*a*) Combined Lick and MMT spectra of the core region. The emission lines of C IV, He II, C III], and N V are marked. (*b*) Spectrum in a 3″ region centered on the southern radio knot, a distance 3″.5 south of the core. These spectra illustrate the differing ionization states in the two regions of the cloud.

The initial long-slit spectra, taken in 1987 May, were of rather poor quality because of very bad seeing. Nonetheless, the spectra clearly showed the Lyα emission to be quite extended and to possess a strong velocity gradient. While these observations provided the impetus for the intensive follow-up work, they are of sufficiently low quality that they do not play an important role in our analysis. They are presented in Spinrad (1987) and Djorgovski (1988).

The long-slit observations made in July were done in excellent conditions and will form the bulk of the working data set for the discussion of the spectral and spatial properties of the emission lines. Two integrations of 4000 s duration each were performed on 1987 July 1 and 3 UT with the slit oriented in position angle 190° and centered at $\alpha^* = 34^s.05$, $\delta^* = 39''.0$.

The observing conditions were excellent for these two observations: the seeing was FWHM ~1″, and the city of San Jose was covered with dense fog (suppressing light pollution). These two spectrograms were reduced using standard techniques and were shifted into registration and combined. After sky subtraction, these spectra clearly showed *extended* emission lines of C IV λ1550, He II λ1640, and C III] λ1909. These emission features are seen in the two observations separately, as well as in the MMT spectra of 1987 June, and thus are solidly confirmed. Furthermore, these spectra show the complex velocity fields of Lyα and the other emission lines. As will be discussed below, perhaps the most striking result is that the velocity fields of C IV, C III, and He II are *systematically* different from that of Lyα.

The observation of 1987 July 2 UT was made with the slit oriented in position angle 210° and centered on the position of the southern radio knot, $\alpha^* = 34^s.0$, $\delta^* = 37''.0$. The observing conditions were less favorable for this observation, and we failed to detect the high-ionization metal lines convincingly. The crucial factor in the detection of these features may be minimizing the scattered light from the K star. Similar remarks apply to the data obtained on 1987 July 27 UT.

A spectrum of the K star 10″ to the west was obtained on 1987 July 1, just after the observations of 3C 294. The observations were made with the same instrumental parameters, including the position angle of the slit, as for the observations of 3C 294. These data were used to remove the scattered light of the star from the spectra of 3C 294. The integration time for this observation was 300 s.

The individual raw two-dimensional spectrograms were bias-subtracted and divided by the sum of 25 individual flat-field exposures. Two regions of the slit, on either side of the Lyα emission, were used to determine the intrinsic sky spectrum. The average sky was then subtracted from the entire frame. Cosmic-ray detections, which can be recognized as being single-pixel events, were removed and replaced by the median of the surrounding 10 pixels. The spectrograms from 1987 July 1 and 3 were registered, using a star near the end of the slit, and were co-added. Individual single-column spectra were then extracted for the entire region of the slit where Lyα was visible, plus 5 columns further on either side.

Before fluxing the one-dimensional spectra, each was aver-

aged with its nearest neighbors (one to each side) with weighting factors of 1:2:1. This effectively smooths the data without compromising either the spectral or spatial information significantly. This averaging was necessary because of the rather low intrinsic signal-to-noise ratio of the data. Each one-dimensional spectrum was then wavelength-calibrated, corrected for atmospheric extinction, and fluxed using the observations of the standard stars.

The spectrum of the K star was processed and calibrated in the same manner to produce a single high signal-to-noise ratio spectrum of the star for removal of the scattered light from the individual spectra of 3C 294. This was done by scaling the spectrum of the K star in such a way that the amplitude of the spectral break at 4000 Å had the amplitude observed in the individual uncorrected spectra of 3C 294. This amplitude will, of course be different for each individual spectrum. A further complication arises from the effects of atmospheric refraction. The amount of K star light that falls on the slit will be wavelength-dependent. This effect should be small because the star is 10″ away, farther than the typical refraction distance (Filippenko 1985), and so we have not attempted to apply any correction.

After each spectrum had been fully processed, we analyzed the emission lines. Gaussians were fitted to each of the emission lines, Lyα, C IV λ1550, He II λ1640, and C III λ1909, for each spectrum. We also simultaneously determined the level of the continuum in two 50 Å bands on either side of Lyα. The results of this analysis, the velocity fields, variations in line widths, and surface brightness in each line, are presented in Figures 4*a*, 4*b*, and 4*c*.

To allow a better comparison of the spatial properties of Lyα and the other lines, rather than their best-fitting Gaussians, we also produced two-dimensional "phase-space" diagrams (maps of intensity in a position versus velocity plane). This was done by cutting out a small portion (50 × 50 pixels) of the sky-subtracted two-dimensional spectrogram around Lyα and C IV λ1550. Special care was taken to ensure that the velocity zero points for each frame were the same. In the figures that follow, we choose the velocity of Lyα at the radio core as our zero point. The kinematic and spatial properties of He II λ1640 and C III λ1909 appear to be the same as those of C IV λ1550, but with less signal-to-noise, so we will concentrate our discussion on C IV λ1550. The spatial profile of the scattered light from the K star was determined by summing over 20 pixels blueward and redward and averaging the profiles. A two-dimensional template was then constructed and subtracted from each 50 × 50 frame to remove the starlight. This procedure effectively removes the scattered light locally, much in the same way that the sky is subtracted. Any continuum associated with 3C 294, however, is also removed by this technique. To compare the absolute velocity fields of Lyα and C IV λ1550, we expanded the Lyα frame in the direction of the dispersion in such a way that it has the same velocity range as the C IV frame. Contour plots of the resultant "phase-space" maps are shown in Figure 5 and will be discussed below.

III. DISCUSSION

There are a number of issues which can be discussed on the basis of our data concerning 3C 294 and similar distant radio galaxies. Because of its high redshift and substantial look-back time (64% of the Hubble time for $q_0 = 0$), one can address issues pertaining to the early evolution of massive stellar systems. Related to this are the questions of the origin, ionization, and dynamics of the gas. We also discuss the importance of the radio activity on its environment and relevance of this object to other classes of active galaxies.

Our assumed cosmology ($H_0 = 50$ km s^{-1} Mpc^{-1}, $q_0 = 0$, $\Lambda = 0$) maximizes sizes and luminosities. At the redshift of 3C 294, this results in a length scale of 1″ = 12.8 kpc, a look-back time of 12.6 Gyr, and a distance modulus (for magnitudes proportional to logarithms of f_ν) of $m - M = 45.4$ (46.5 for total luminosities). For $H_0 = 50$ and $q_0 = \frac{1}{2}$ the length scale and look-back times are 8.5 kpc and 10.3 Gyr, respectively; absolute magnitudes and luminosities are reduced by a factor of 2.3.

a) Origin of the Optical and Near-IR Continuum

While our information concerning the continuum of 3C 294 is severely constrained by the presence of the foreground star, we are able to make a rough determination of its spectral energy distribution. The central issue concerning the continuum in this and other high-redshift radio galaxies is the nature of the source. The shape of the spectral energy distributions (SEDs), the small scatter in the *K*-band Hubble diagram (Lilly 1989), and the photometric continuity with lower redshift objects are fairly compelling evidence in favor of a stellar origin for the optical and near-IR continua. Recently, however, there have been reasons to question this interpretation and reconsider nonstellar sources. Among these are the strong spatial alignment between the continuum and radio axes and, more recently, the reports of strong polarization of the optical continuum (di Serego Alighieri *et al.* 1988; Scarrott, Rolph, and Tadhunter 1990). In Table 2 we give the continuum magnitudes (or upper limits) that we have measured for 3C 294 and their corresponding flux densities in cgs units. In Table 3 we compare the photometric properties of 3C 294 with other radio galaxies at similar redshifts.

As stated above, we have failed to detect the continuum in our optical images, our upper limit for an unresolved object

TABLE 2

EMISSION-LINE STRENGTHS

Line	3C 294[a]	H II Region[b]	Shocks[c]	Power Law[d]
Lyα	100	100	100	100
N V λ1240	2	...	8×10^{-4}	0
C IV λ1550	10	10.7	7.7	3.9
He II λ1640	10	...	0.78	4.1
C III] λ1909	12	7.2	7.45	9.2

[a] Inner 4″ centered on radio core position.
[b] From Stasinska 1984, for $T_{\rm eff} = 55{,}000$ K, $Z/Z_\odot = 0.2$.
[c] From Shull and McKee 1979, model E, $V_{\rm shock} = 100$ km s^{-1}.
[d] From Ferland 1981, for $\alpha = -1.5$, $\log U = -2.5$, $Z/Z_\odot = 0.3$.

TABLE 3

PHOTOMETRIC AND EMISSION-LINE PROPERTIES OF HIGH-REDSHIFT RADIO GALAXIES

Object	z	Magnitude (band)	Continuum Flux Density ($\lambda_{\rm rest} = 1330$ Å) (μJy)	L(Lyα) (ergs s^{-1})
3C 239.....	1.781	21.6 (*R*)	2.4	2×10^{44}
3C 256.....	1.819	21.6 (*R*)	2.6	5.2×10^{44}
4C 40.36.....	2.269	21.7 (*R*)	1.9	5×10^{44}
3C 326.1.....	1.825	23.5 (*R*)	0.5:	3.6×10^{44}
3C 294.....	1.786	$\gtrsim 22$ (*V*)	2.5	7.6×10^{44}

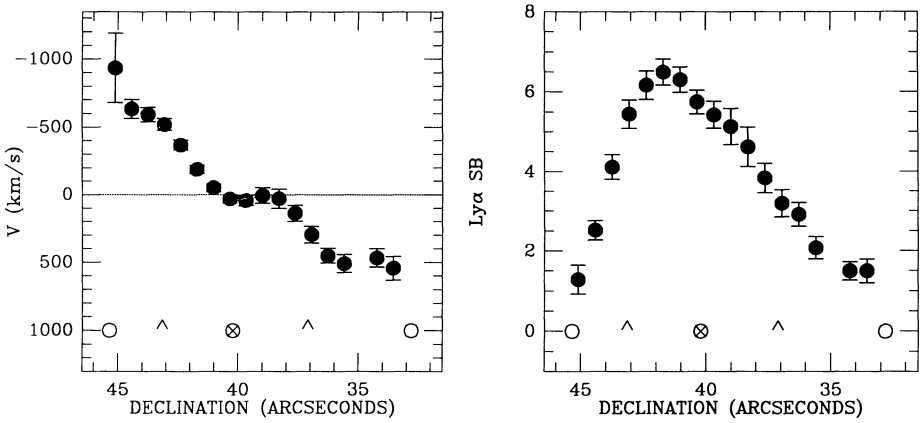

FIG. 4*a*

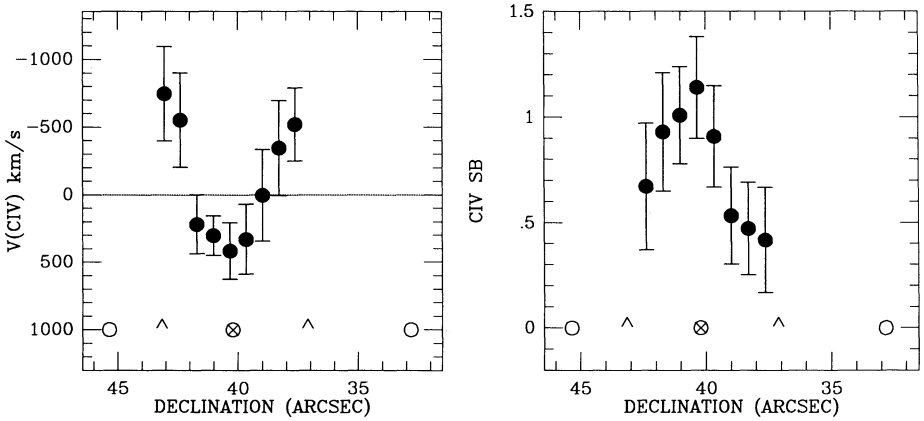

FIG. 4*b*

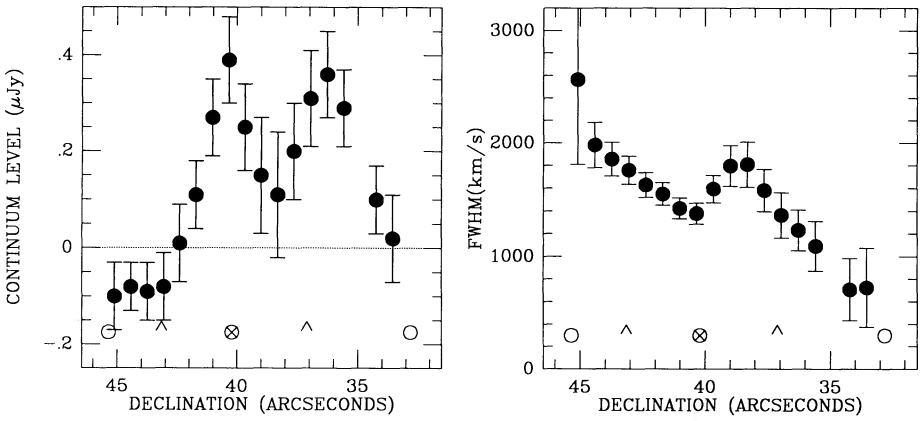

FIG. 4*c*

FIG. 4.—Multipanel presentations of the velocity-integrated properties of the emission lines from the long-slit spectra taken in position angle 180°. In each panel the *x*-coordinate is the declination (δ*) and the features in the radio map have been indicated with the following symbols: core (*circled crosses*), knots (*carets*), and lobes (*open circles*). In each case, the error bars shown are $\pm 1\ \sigma$. (*a*) The surface brightness profile and the velocity field of Lyα. (*b*) The surface brightness profile and the velocity field of C IV λ1550. (*c*) The surface brightness profile of the continuum and the Lyα line widths.

being $m_{AB3500} > 20.2$ mag or $M_{AB1250} > -25.2$ at the redshift of 3C 294. A much more sensitive measurement of the rest-frame UV flux comes from our long-slit spectra, where we detect the continuum directly. We have removed the scattered light from the K star as described above. The error bars on the continuum flux density shown in Figure 4*c* reflect the uncertainty in the continuum level after the scattered light has been removed. The actual uncertainty in the continuum level may be dominated by error in the scattered-light correction and is likely to be somewhat larger. Our derived continuum profile along the slit is shown on the left-hand panel of Figure 4*c*. Each of the two knots shown in Figure 4*c* has a flux density ~ 1.25 μJy, corresponding to *U*-magnitudes of 22.9 ± 0.5 (or $U_{AB} \approx 23.6$), and both appear to be slightly resolved along the

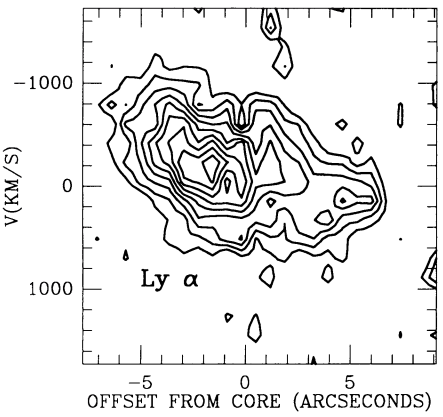

FIG. 5a

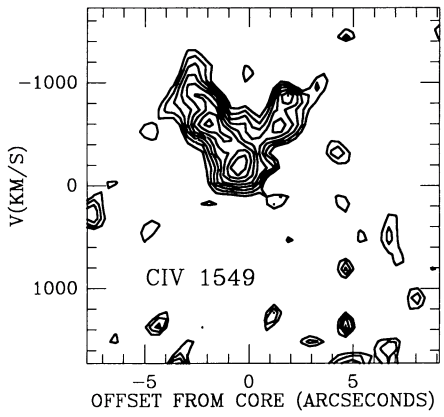

FIG. 5b

FIG. 5.—Phase-space representations of the long-slit spectrograms of (*a*) Lyα and (*b*) C IV λ1550. The *x*-coordinate in each is the declination (δ*). The two panels have the same velocity range and the same velocity zero point. The zero point was chosen to be the velocity of Lyα at the position of the radio core.

slit. The northern of the two knots is spatially coincident, within the measurement errors, with the radio core and thus may be identified with the nucleus of the galaxy. The *U*-magnitude of 22.9 translates to an absolute magnitude $M_U = -22.5$, or $M_{AB1250} = -21.8$ in the galaxy rest frame. Using the spectrum of the core region presented in Figure 3*a*, we determine a continuum flux density corresponding to a *V*-magnitude $\gtrsim 22$ in a $2'' \times 5''$ aperture. This corresponds to an absolute magnitude of $M_V \approx M_{AB1970} \gtrsim -23.4$. Although we believe that we detect the *V* continuum spectroscopically, the magnitude derived should be treated with caution because of the uncertainty in removing the scattered K star light. We will regard it as an upper limit to the true value. Taken at face value, this *V*-magnitude is quite comparable to those of other 3CR radio galaxies at $z \sim 2$.

The spectrum of the inner regions shown in Figure 3*a* shows that the continuum is flat longward of 1500 Å (rest) and declines as one goes blueward of 1500 Å. This continuum shape is characteristic of the $z \sim 2$ radio galaxies as shown by Chambers and McCarthy (1990) and is indicative of a declining star formation rate. The change in continuum slope at 1500 Å is observed at 4180 Å, and thus may be contaminated by the 4000 Å discontinuity in the spectrum of the foreground K star. There is no obvious feature at 4000 Å in the scattered-light–corrected spectrum, but we cannot say with confidence that we have removed all of the scattered light longward of 4000 Å. Our detection (or upper limit) of the *V*-band continuum from the radio core region, when combined with the *K*-band photometry (§ IIc, and see below) implies a $V-K$ color of 4 or greater. If both the *V*-band and the *K*-band light are stellar in origin, the large $V-K$ color implies that the core region had a larger star formation rate in the past. This is consistent with the down-turn in the continuum slope shortward of 1500 Å (rest).

At longer wavelengths we detect the continuum with a much higher degree of confidence. As stated above, we measure $K = 18.0 \pm 0.3$ (or $K_{AB} = 19.9$) and $J = 21.0 \pm 0.4$ (or $J_{AB} = 21.8$). This *K*-magnitude is quite typical for its redshift and falls very close to the mean *K*-*z* Hubble relation given by Lilly (1989). The $J-K$ color of 3 ± 0.5, however, is extremely red, although poorly determined. At a redshift of 1.786, the rest-frame wavelengths of the half-power filter transmission points are 4010 and 5020 Å for *J* and 7110 and 8380 Å for *K*. Thus there may actually be excess [O III] λ5007 emission contributing to *J*, but no plausible strong emission line at *K*, making the $J-K$ color potentially even redder than 3. The next reddest $J-K$ color of which we are aware for a radio galaxy is 2.4 for 3C 356 at $z = 1.08$ (Eisenhardt and Chokshi 1990). It is difficult to reproduce such a red color with stellar models. The reddest Bruzual model, a 1 Gyr single-burst model starting at $z = 100$, gives $J-K = 2.0$ at $z = 1.8$, but is far too red in $V-K$ and $U-K$ to match 3C 294 or other high-redshift radio galaxies. Ascribing this red color to a power-law continuum requires a spectral index of -3, much steeper than observed in quasars (Neugebauer *et al.* 1979). A modest amount of reddening due to dust (a few tenths E_{B-V} in the 3C 294 rest frame) could produce the observed $J-K$ color from reasonable stellar or nonthermal SEDs, but this would drastically redden the $V-K$ and $U-K$ colors (by several magnitudes), making the observed spectrum still more difficult to account for. One might appeal to a two-component model in which the *J* and *K* light arises from a reddened old stellar population and the rest-frame UV light arises from a younger, dust-free population, although such a scenario may seem contrived. Small amounts of dust may also strongly quench Lyα emission, although one might appeal to special circumstances in the relative distributions of dust and gas to preserve the high Lyα luminosity. In short, for either the stellar or power-law cases it seems difficult to reconcile the red $J-K$ colors with the apparent flatness of the rest-frame UV spectrum. A stellar origin of the IR and UV light seems favored by the spatial extension of the image, the *K*-band magnitude, and, to a lesser degree, the shape of the SED. Until a better determination of the SED is available, however, it is premature to draw any strong conclusions regarding the stellar populations from the present data.

We can determine an upper limit to the current star formation rate from the observed Lyα luminosity by assuming that all of the Lyα arises from photoionization by hot stars. After converting the Lyα luminosity to the corresponding Hα luminosity, assuming the case B ratio Lyα/Hα = 8.74, and applying the relation between *L*(Hα) and the star formation rate from Kennicutt (1983), we estimate a star formation rate of 120 $M_\odot$ yr^{-1}, for stars with $M > 10\ M_\odot$. A normal initial mass function then implies a total star formation rate of 760 $M_\odot$ yr^{-1}. These rates should be taken as upper limits, since they assume that all of the Lyα emission results from stellar photoioniza-

tion. The shape of the observed continuum, however, implies that only about half of the Lyα emission can arise from photoionization by stars (Chambers and McCarthy 1990).

b) Physical Conditions in the Radio-emitting Plasma

In this section we will briefly discuss the physical parameters in the radio-emitting plasma, subject to a number of usual assumptions (e.g., Miley 1983): (1) the radio emission is due to synchrotron emission, (2) the total energy of a component is minimal as a function of magnetic field strength, (3) the relativistic electron and proton energies are equal, (4) the filling factor of the synchrotron emission is unity, and (5) the nonthermal spectrum is a (straight) power law extending from 10 MHz to 100 GHz. We also assume that the spectral index $\alpha \sim -1.1$ (Kellermann, Pauliny-Toth, and Williams 1969) of the integrated radio emission applies to all individual components.

We derive for the compact, highest surface brightness region a magnetic field strength $B \approx 6.1 \times 10^{-4}$ G, a (minimum-energy) pressure $P_R/k \sim 2.5 \times 10^8$ K cm^{-3}, and a lifetime of relativistic particles (radiating at a rest-frame frequency of 5 GHz) against synchrotron and inverse Compton losses of $\sim$15,000 yr. This assumes that the peak flux density (92.1 mJy at 5 GHz) originates in a sphere of radius $\sim$0.″2 (2.5 kpc).

Similarly, for the diffuse, low-brightness radio emission along the northwestern edge of the southern lobe, we derive a magnetic field strength $B \sim 6.4 \times 10^{-5}$ G, a minimum-energy pressure $P_R/k \sim 2.8 \times 10^6$ K cm^{-3}, and a lifetime of relativistic particles (radiating at a rest-frame frequency of 5 GHz) against synchrotron and inverse Compton losses of $\sim$40,000 yr. This assumes an average surface brightness of 0.13 mJy beam^{-1} at 5 GHz, with a beam size of 0.″4 × 0.″4 and a line of sight through this medium $\sim$1″ (12.8 kpc).

c) Mass and Density of the Gas

We begin our discussion of the physical properties of the emission-line gas with an estimation of the density and the total mass of the gas. The large redshift and apparent faintness of this object render most of the standard emission-line nebular diagnostics useless, preventing us from determining the electron density or temperature directly. Instead we must attempt to constrain these by indirect means. As we will show below, the bulk of the ionized gas in the inner 60 kpc must be heated by a photoionization process rather than by collisional ionization. We will analyze the emission-line properties of the cloud in this perspective.

The Lyα luminosity for pure case B recombination at $T = 10^4$ K is given by

$$L_{\mathrm{Ly}\alpha} = 4 \times 10^{-24} n_e^2 f_v V \text{ ergs s}^{-1} ,$$

where f_v is the volume filling factor of the gas and V is the total volume. In terms of the Lyα luminosity, the volume, and the filling factor, the density is

$$n_e = \tfrac{1}{20}(L_{44}/f_v V_{70})^{1/2} \text{ cm}^{-3} ,$$

where L_{44} and V_{70} are respectively the Lyα luminosity in units of 10^{44} ergs s^{-1} and the total volume in units of 10^{70} cm^3. The total mass of ionized gas is then

$$M(\mathrm{H\ II}) = 10^9 (f_{-5} L_{44} V_{70})^{1/2} M_\odot ,$$

where f_{-5} is the filling factor in units of 10^{-5}. Thus, in order to determine the total mass of gas, we must know either the density or the volume filling factor. We will use three approaches to estimate these parameters. The first is to assume that the filling factor of the 10^4 K gas is similar to that determined for emission-line gas associated with radio galaxies at low redshifts. The second is to attempt to determine the density from the ionization state. The third approach assumes pressure balance with the radio-emitting plasma.

There are a number of low-redshift radio galaxies with extended line emission whose densities can be measured directly from the [S II] lines at 6720 Å (e.g., Heckman, van Breugel, and Miley 1984). These objects have a fair dispersion in f_v, but most lie in the range $\sim 3 \times 10^{-4}$ to 10^{-5}. Emission-line nebulae associated with cooling flows typically have $f_v \sim 2 \times 10^{-6}$ (Heckman *et al.* 1989). We will adopt a value of 10^{-5} as a guess. Using a characteristic radius equal to the Lyα half-light radius of 3″ and the total Lyα luminosity of 7.6×10^{44} ergs s^{-1}, the density and total mass are then 50 cm^{-3} and $2.3 \times 10^9 M_\odot$, respectively. These values are moderately sensitive to our more or less arbitrary assumption regarding f_v.

An alternative approach makes use of the ionization parameter U:

$$U = Q_{\mathrm{ion}}/4\pi r^2 n_e c ,$$

where Q_{ion} is the ionizing photon flux. We use the power-law models of Ferland and Osterbrock (1986) to estimate U from the observed strengths of C IV λ1550, He II λ1640, and C III λ1909 (see Table 2). The models fit best for log $U = -2.5$ for a power law with index $\alpha = -1.5$. To determine the flux of ionizing photons, Q_{ion}, we can either count the number of Lyα photons and assume case B, or we can extrapolate the observed continuum as a power law. These two methods give roughly the same result (see § III*f*), $Q_{\mathrm{ion}} \approx 4 \times 10^{55}$ photons s^{-1}. The gas density is then $n_e \sim 2$ cm^{-3}, again at a characteristic radius of 3″ $= 10^{23}$ cm. For this density the volume filling factor is $f_v \sim 8 \times 10^{-4}$ and the total H II mass is $10^{10} M_\odot$. The density derived from this approach should be considered as a lower limit. If the ionizing continuum is not emitted into a full 4π steradians, as we will argue may be the case, then higher densities are required to maintain the ionization parameter.

The third approach involves estimating the pressure in the diffuse radio plasma. As we discussed above, the minimum-energy pressure in the diffuse radio emission (southern lobe) is of the order of 3×10^6 K cm^{-3}. If the 10^4 K gas that is spatially coincident with this radio emission is in pressure equilibrium with it, the electron density of the thermal gas is then $\sim$150 cm^{-3}. This is quite high and is likely to represent an upper limit on the pressure in the 10^4 K gas.

These three approaches to estimating the density of the thermal gas are each uncertain by more than an order of magnitude, and the spread in the derived densities is two orders of magnitude (2–150).

d) Dynamics and Energetics of the 10^4 K *Gas*

The velocity fields of Lyα and C IV are shown in Figures 5*a* and 5*b*. As Figure 5*a* shows, there is a large, smooth velocity gradient in the Lyα emission. The total amplitude of the Lyα velocity field is 1500 km s^{-1}, and the maximum rate of shear is $\sim$8 km s^{-1} kpc^{-1}. The typical FWHM of Lyα is $\sim$1400 km s^{-1}, or $\sigma = 500$ km s^{-1}. These large line widths may be the result of turbulent motion or shear along the line of sight. Before we can draw any conclusions from the kinematic data, however, we need to know whether the motions are driven by gravity, or if they result from hydrodynamic interactions

between the outflowing radio plasma and the thermal gas. A third possibility, that some component of the Lyα line width and velocity gradient arises from optical depth effects, is discussed in § III*g*.

If the gas motions are driven by gravity, we can estimate the enclosed virial mass. While the smoothness and north-south symmetry of the velocity field are certainly suggestive of rotation or infall/outflow, the actual motions may be more complex. Irrespective of the details of the kinematics, the virial mass interior to 60 kpc is of order

$$M = 3 \times 10^{12} R_{60} V_{500}^2 M_\odot ,$$

where R_{60} is the radius of the system in units of 60 kpc and V_{500} is the velocity dispersion in units of 500 km s^{-1}. This mass is quite reasonable for a large galaxy or a small group and is comparable to the mass of M87 interior to similar distances (Fabricant and Gorenstein 1983). The amplitude of the Lyα velocity field increases linearly with R over most of the region of detectable signal. There are a number of other high-redshift radio sources with extended emission lines having simiar kinematic properties. Two examples are the $z = 1.21$ radio galaxy 3C 324 (Spinrad and Djorgovski 1984*a*) and the $z = 0.56$ quasar 3C 275.1 (Hintzen and Stocke 1986). The latter of these has been interpreted as undergoing solid-body rotation (Hintzen and Stocke 1986). A solid-body rotation curve requires a uniform mass density throughout the cloud, which seems rather implausible, both on theoretical grounds and in light of the central concentration of the Lyα emission. A "solid-body rotation" curve, however, can also be produced by infall or outflow.

Kinematic arguments similar to those outlined above can be applied to the line widths. Assuming that the velocity dispersion of the Lyα–emitting gas is representative of the material that constitutes the bulk of the mass, the total kinetic energy is then of order

$$\mathrm{KE} = 2.5 \times 10^{60} M_{12} \sigma_{500}^2 \text{ ergs} ,$$

where M_{12} is the total mass in units of 10^{12} $M_\odot$, and σ_{500} is the velocity dispersion of the gas in units of 500 km s^{-1}. As discussed above, the mass of gas probably lies in the range 10^9–10^{11} $M_\odot$. The kinetic energy of the 10^4 K gas alone is then in the range 10^{57}–10^{59} ergs. Cloud-cloud collisions can convert this kinetic energy into UV photons, and ultimately into Lyα photons. Given the Lyα luminosity of 7.6×10^{44} ergs s^{-1}, one derives a lifetime of

$$\tau = 3 \times 10^6 \, \mathrm{KE}_{58} L_{44}^{-1} \epsilon \text{ yr} ,$$

where ϵ is the efficiency factor and KE_{58} is the kinetic energy in units of 10^{58} ergs. If the efficiency is modest, $\epsilon \sim 10^{-2}$, then the dissipation time is quite short ($\sim 10^4$ yr) and the system must be dynamically reheated. This suggests that some continuous input of energy is required to maintain the velocity widths of the lines, rather than a one-time injection that would arise from a single event (e.g., a merger). Hydrodynamic interactions between the radio-emitting plasma and the thermal gas are a natural source of energy input.

It is worthwhile at this point to compare the kinematic properties of 3C 294 to low-redshift radio galaxies and cooling-flow nebulae. A number of low- and intermediate-redshift radio galaxies and quasars with extended emission-line regions show large-amplitude velocity fields, although on significantly smaller spatial scales (e.g., 4C 29.30, van Breugel *et al.* 1986; PKS 2152−69, Danziger and Focardi 1988). The line widths in the extended emission lines can be moderately large, particularly at sites of strong radio emission (e.g., 3C 277.3; Heckman, van Breugel, and Miley 1984). The kinematics of emission-line filaments in cooling-flow clusters, however, are quite quiescent. The large-scale velocity fields in cooling-flow nebulae have typical amplitudes of $\Delta V = 100$–200 km s^{-1} (Heckman *et al.* 1989). There is a substantial amount of turbulent motion implied by the line widths, with typical velocity dispersions being $\sigma = 100$–200 km s^{-1} in the inner few hundred parsecs. Thus it appears that the kinematic properties of 3C 294 are more closely related to present-day radio galaxies than to the emission-line filaments associated with present-day cooling-flow clusters.

One aspect of the kinematic data that is not easily understood in this picture is the velocity field of the high-ionization lines. Clearly, the large blueward shear in the C IV emission line south of the nucleus cannot both be the result of rotation or infall *and* sample the same region as the Lyα emission.

This leads us to consider an alternative picture in which the gas motions are the result of hydrodynamic interactions with outflow from the nucleus rather than gravitationally driven rotation. Additional motivation for such a model comes from the strong spatial alignment between the radio source axis and the emission-line gas, and the observation that many low- and intermediate-redshift radio galaxies show comparable velocity gradients in ionized gas associated with radio jets and hot spots (see van Breugel 1986 and Fosbury 1986 for reviews).

It is unclear whether or not the large-scale coherent velocity field can be the result of interactions between the jet and the thermal gas. Analytic calculations by De Young (1986) show that mass entrainment rates for "Cygnus A"-type sources can range from 1 to 300 $M_\odot$ yr^{-1}. One would expect that as ambient gas is entrained into the jet, its velocity increases up to the point at which the gas is shocked and heated and no longer produces significant line emission. Alternatively, the line emission could arise from cool clouds that have condensed and dropped out of the flow. Detailed modeling is required to investigate whether or not the systematic velocity field that we observe can be the result of entrainment.

The north-south symmetry in the radial velocity field can easily be understood in this picture as simply being an inclination effect, with the northern side of the radio source pointing out of the plane of the sky and the southern side pointing into it. The velocity field of the high-ionization lines is still difficult to understand in this picture, but it is conceivable that entrainment could produce a multiphase medium with differing velocity fields and ionization levels.

We are currently unable to determine which of these two processes, mass entrainment or rotation/infall, is the dominant mechanism in producing the observed velocity field. The mass implied by rotation is plausible, but the shape of the velocity field is difficult to understand. The details of the mass entrainment process in jets are poorly understood, and thus one cannot draw many conclusions from the shape of the velocity field in this picture without detailed modeling.

e) Origin and Confinement of the 10^4 K *Gas*

Understanding the origin and confinement of the 10^4 K gas is clearly important. The relationship between the Lyα–emitting gas and the hot gaseous coronae of present-day giant galaxies and clusters is an important outstanding issue.

The question of the origin of extended line-emitting gas in nearby radio galaxies has been discussed by a number of

authors (e.g., Heckman, van Breugel, and Miley 1984; van Breugel *et al.* 1986; Baum and Heckman 1989*a*). In these low-z objects the natural sources of cool gas are the interstellar medium of the host galaxy (or its companions), and the hot (10^8 K) coronae of clusters and giant elliptical galaxies.

The large spatial scale of the Lyα emission for 3C 294 argues that the gas is not simply the interstellar medium of an otherwise developed galaxy. Alternatively, it is possible that the 10^4 K gas is infalling material that will eventually become part of the interstellar medium of the host galaxy. The presence of emission lines of heavy metals (e.g., C IV) requires that at least some fraction of the gas has been cycled through massive stars.

Another possibility is that the gas is related to the hot atmospheres observed in clusters of galaxies at small and intermediate ($z < 0.5$) redshifts. This is attractive on a number of grounds. First, the gas in cluster atmospheres has abundances about one-half of solar. Second, the scale of the Lyα emission can be easily accommodated. What is not clear is whether the 10^4 K gas that we observe at $z \sim 2$ is material that has cooled out of the hot atmosphere (i.e., a cooling flow) or is material that will eventually *become* a part of the hot component. Third, a hot medium can confine the thermal gas, and perhaps the radio source as well. As discussed above, the gas density probably lies in the range $n_e \sim 1$–100 cm^{-3}. Assuming a temperature of 10^4 K, the implied pressure is in the range $nT \sim 10^4$–10^6. Pressures larger than $\sim 10^5$ may require confinement to prevent dissipation on short time scales and have been used as a criterion for detecting high-redshift cooling flows (Fabian *et al.* 1986; Fabian *et al.* 1987). This argument depends strongly on the size of emission-line clouds and the assumptions used in deducing them (e.g., Crawford *et al.* 1988). The pressures and other emission-line cloud parameters that we derive are sufficiently uncertain that we cannot apply the approach used by Fabian *et al.* (1987) with any confidence.

Some constraints on a hypothetical hot medium may be obtained from the radio data. We assume that the *diffuse*, low surface brightness radio emission associated with the southern lobe has fully expanded and is confined by static thermal pressure in a hot corona. Then $P_R/k = 2.8 \times 10^6 = 2n_e T$ (K cm^{-3}) (fully ionized hydrogen). The observed emission-line gas (Lyα) could be in pressure equilibrium with this, since for $T \sim 10^4$ K, $n_e = 100$ cm^{-3}. The hot intercloud medium, in which this emission-line gas is embedded, can be expected to have a temperature of 10^7–10^8 K, typical of cluster halos. If this is in pressure equilibrium with the diffuse radio emission, then n_e(hot) ~ 0.1–0.01 cm^{-3}. The total mass of the hot component, then, is of the order a few times 10^{10}–10^{11} $M_\odot$, consistent with the limit on the dynamical mass from § III*d*. These estimates of the density and mass of the hot medium are very crude, but are consistent with present-day X-ray luminous cluster atmospheres. Evidence for a two-phase medium surrounding other high-redshift radio galaxies comes from observations of the polarization and Faraday rotation structure of the radio sources (Pedelty *et al.* 1989*a*, *b*).

The pressure in the high surface brightness northern hot spot is $P_R/k = 2.5 \times 10^8$. It is unlikely that this component is thermally confined, since this would require implausibly high thermal gas pressures. Instead, ram pressure on the advancing hot spot by the hot ambient gas is more likely. For an ambient gas density of 0.1–0.01 estimated above, we derive advance speeds for the northern hot spot of $v_H \sim 4500$–$14{,}000$ km s^{-1} (0.015–$0.05c$). These velocities are somewhat lower than those derived for local high-luminosity sources (e.g., Myers and Spangler 1985; Alexander and Leahy 1987). This would lead to an estimate for the age of the source of $\sim 6 \times 10^6$ to 1.8×10^7 yr, again a reasonable number when compared with current beam-propagation models (e.g., Gopal-Krishna and Wiita 1987). In conclusion, it is possible to construct a consistent model of a clumpy, two-phase medium as in other emission-line radio galaxies.

There are a number of similarities between the 3C 294 Lyα emission-line cloud and the nebulae associated with cooling flows. The equivalent widths of Lyα in cooling-flow clusters are as large as in the radio galaxies (~ 300 Å; Hu 1988). The Lyα luminosity of the 3C 294 cloud is, however, two orders of magnitude larger than those of the most luminous nearby cooling-flow nebulae (e.g., A1795; Norgaard-Nielsen, Jorgensen, and Hansen 1984). Fabian and coworkers (e.g., Fabian *et al.* 1986) suggested that the nebulae associated with powerful 3CR radio galaxies at large redshifts are massive cooling flows. Naturally, there are some difficulties involved in such a model. As discussed above, the mass of 10^4 K gas probably lies in the range 10^8–10^{11} $M_\odot$. This is two or more orders of magnitude larger than the most massive cooling-flow nebulae observed locally (Heckman *et al.* 1989). The emission line spectra of cooling-flow nebulae observed locally closely resemble shock-heated gas (Hu, Cowie, and Wang 1985; Heckman *et al.* 1989; but see Robinson *et al.* 1987). As will be shown below, we can rule out shock heating as the dominant ionization mechanism in the inner regions of 3C 294. Additional sources of ionization, from either massive stars or an active nucleus, could act independently of a cooling flow. Mass-flow rates estimated from the observed Lyα emission, assuming no reionization, are quite large, $\sim 10^5$ $M_\odot$ yr^{-1}. These rates are meaningless if the gas is photoionized by a central source, as we will argue below.

Perhaps the greatest difficulty in a cooling-flow model for 3C 294 lies in the small amount of time in which the cooling flow must form. In the most optimistic cosmology ($H_0 = 50$, $q_0 = 0$) the age of the universe at $z = 1.8$ is 7 Gyr. If most giant elliptical galaxies formed at $z \gtrsim 5$, as suggested by the work of Hamilton (1985) and Lilly (1989), then the time since galaxy formation, and hence the time of enrichment of the gas, is 3 Gyr. For an $\Omega_0 = 1$ universe the time since galaxy formation is only 1 Gyr. Most cooling-flow clusters observed locally have cooling times of 14 Gyr ($H_0 = 50$), nearly three-fourths of the Hubble time; see e.g., Hu, Cowie, and Wang (1985), who for this reason argue that one should not expect to find many active cooling flows at redshifts larger than ~ 0.2. Fabian *et al.* (1986) argue that the buildup of massive clusters through mergers of smaller subunits has resulted in increased cooling times in present-day massive clusters. They suggest that poorer clusters with short cooling times, and hence cooling flows, should be more prevalent at high redshift.

f) *Ionization of the* Lyα *Cloud*

Before we consider the source of ionizing photons, we briefly show that collisional ionization is unlikely to be significant. The spectrum in Figure 3*a* shows that, as in many of the high-redshift radio galaxies (Spinrad and Djorgovski 1984*b*; Spinrad *et al.* 1985), the relative strengths of C IV λ1550 and He II λ1640 are roughly equal. This is quite at odds with the shock models of Shull and McKee (1979). In all of their models in which C IV λ1550 has a significant strength, it is roughly 10 times stronger than He II λ1640 (see Table 2). In their metal-depleted model He II is stronger relative to C IV, but is still a factor of ~ 3 too weak. The shock models of Shull and McKee,

and the metal-depleted model in particular, predict N V/Lyα ratios that differ by more than an order of magnitude from the observed ratio. Furthermore, the nonequilibrium shock models of Hartigan, Raymond, and Hartmann (1987) also fail to reproduce the observed He II and N V line strengths. Thus it seems that shock ionization, at least in the inner regions where C IV and He II are strong, is not the dominant ionization process.

Turning to photoionization, we now consider whether the observed continuum is adequate to ionize the observed Lyα–emitting gas. This can be estimated by extrapolating the continuum to wavelengths shorter than 912 Å, using models appropriate to either a stellar or power-law source. As was noted in § III*a*, the 4×10^8 year old Bruzual models used by Chambers and McCarthy (1990) to match the observed UV continuum of radio galaxies can produce roughly half of the observed Lyα flux; models with more hot and massive stars may result in more ionizing photons, but even O5 stars alone have a factor of 2.5 flux decrement below 912 Å. Thus a substantial fraction, but perhaps not all, of the large observed Lyα luminosity may be provided by stellar ionization.

For the power-law case we use an index of $\alpha = -1$ ($f_\nu \sim \nu^\alpha$) and a high-energy cutoff at 4 rydbergs. From the continuum profile in Figure 4*c* we determine that the spatially integrated flux density at 1250 Å is 2.5 μJy. The ionizing photon flux is then 3.7×10^{55} photons s^{-1}. The Lyα luminosity integrated over the entire cloud is 7.6×10^{44} ergs s^{-1}, requiring an ionizing photon flux of 4.7×10^{55} photons s^{-1}. Thus, if the observed continuum were nonstellar, it could produce roughly the necessary number of ionizing photons to account for the observed Lyα, provided that the covering factor of the thermal gas is close to unity.

The presence and strength of the high-ionization lines (C IV, He II) provides a constraint on the nature of the ionizing source. The H II region models of Stasinska (1984) produce the observed C IV/Lyα ratio only for effective temperatures of $\sim$55,000 K or greater and for metallicities of $\sim$20% of solar. Such stars are either rare or absent in locally observed H II regions. The "warmer" models of Terlevich and Melnick (1985) can easily produce the observed high-ionization lines, but they too require stars that are hotter than are observed locally. Alternatively, the high ionization lines could arise from Wolf-Rayet stars. WN stars show strong C IV λ1550 and He II λ1640 emission lines, with about equal strengths (e.g., Garmany and Conti 1982). Furthermore, WN stars also show strong N V λ1240, which is also weakly present in our spectra of 3C 294. A number of nearby star-forming galaxies show Wolf-Rayet features in their integrated nuclear spectra (Osterbrock and Cohen 1982; Armus, Heckman, and Miley 1988). W-R stars, however, fail to fully match the observed spectra. They produce moderate emission from N IV λ1718, which is not observed in radio galaxies, and they fail to produce the strong forbidden and semiforbidden lines (e.g., C III λ1909) that are seen in the radio galaxies. Furthermore, stellar populations hot enough to produce the high-ionization permitted lines will also produce a flat spectrum (in f_ν) in the rest frame UV. This is in contrast to the declining spectra observed in 3C 294 and other radio galaxies. Thus the failure of stellar photoionization to match the emission-line ratios and the lack of a flat continuum spectrum in the UV argue that hot stars do not contribute significantly to the ionization for all but the lowest ionization lines.

The alternative interpretation, that the gas is primarily ionized by hard photons from a nonthermal source, is motivated by the wide range of ionization present and the central concentration of the high-ionization lines. In Table 2 we list the observed strengths of emission lines in the region centered on the radio core. We also list the line strengths predicted from various models, including H II regions, power-law photoionization, and radiative shocks. The nonthermal photoionization models are from Ferland and Osterbrock (1986). The $\alpha = -1.5$, $\log U = -2.5$ power-law model reproduces the observed strengths of C IV, He II, and C III] reasonably well. The source of ionizing photons, presumably the nucleus, must be hidden from view in this case, since arguments similar to those given above show that $\sim 10^{55}$ ionizing photons are required. We have cited evidence above that suggests that most of the observed UV continuum is stellar in origin. Furthermore, as Figures 1, 4, and 5 show, there is no signature of the radio core or the central engine that powers it in either the Lyα surface brightness distribution or the Lyα velocity field. The indication from the emission lines that the core is significant comes from the high-ionization emission lines of C IV and He II, both of which have surface brightness profiles and velocity fields that are roughly symmetric with respect to the core. A model in which the high-ionization emission lines are the result of gas photoionized by a nonthermal power-law continuum from the nucleus may require that the ionizing continuum be highly anisotropic. An anisotropic ionizing continuum is also quite attractive for morphological reasons. As described above, the Z-shaped radio structure can be best understood as a result of a change of the outflow axis of the central source. As Figure 4*b* shows, the high-ionization lines are confined to the region between the two radio knots. Furthermore, the overall symmetry axis of the Lyα cloud is skewed with respect to the outer radio source axis, and is closer to, but slightly leading, the inner radio source structure (see Figs. 1 and 2). This is highly suggestive of a picture in which the nucleus emits a pencil beam of ionizing radiation along its spin axis. This radiation beam then ionizes a narrow cone of gas to produce the high-ionization emission lines that we observe. As the spin axis of the central engine precesses, the beam will ionize different regions of the cloud. The large-scale radio emission is produced by material that left the nucleus some $\sim 10^7$ years ago, and hence it tells us where the jet was pointing then. The inner radio source structure then tells us where the beam was pointing at later times, and the emission lines tell us where the beam was pointed only a light crossing time (10^5 yr) ago. In this picture, then, the slight misalignment between the inner radio source axis and the emission-line axis follows quite naturally.

There is supporting evidence for an anisotropic ionizing-beam model from the larger sample of 3CR radio sources and their associated nebulae. The extended emission-line regions associated with local high-luminosity radio galaxies have spectra indicative of nonstellar photoionization (Robinson *et al.* 1987). Depending on the shape of the ionizing continuum, these objects may require more ionizing photons than can be accounted for directly, unless the source of ionization is anisotropic (Robinson *et al.* 1987; Baum and Heckman 1989*b*). The emission-line nebulae surrounding 3CR radio galaxies with redshifts in the range 0.1–1.4 have relative line strengths indicative of power-law photoionization (McCarthy *et al.* 1988). In this redshift range virtually all of the emission-line regions lie along the radio source axes (McCarthy *et al.* 1987*b*; McCarthy and van Breugel 1989). In several cases the emission-line gas lies *beyond* the radio jet working surfaces (hot spots). These

cases suggest that it is the *direction* of outflow (of both photons and relativistic particles), and not the presence of the synchrotron-emitting plasma itself, that is the fundamental parameter in determining the location of the emission-line regions. Such a picture is most easily understood if the ionizing continuum is emitted in a highly anisotropic manner. The alignment of the emission-line regions within 15° of the radio axis suggests that the opening angle of the ionizing photon beam is of the order of 30°. The inferred isotropic photon flux for 3C 294 would then be $\sim 10^{57}$ s^{-1}, similar to that of luminous quasars.

Evidence for anisotropic ionizing radiation in nearby low-luminosity active galaxies is quite strong. In Seyfert galaxies the evidence comes both from imaging spectroscopy of the ionized gas (e.g., Pogge 1988; Wilson, Ward, and Haniff 1988; Tadhunter and Tsvetanov 1989) and from spectropolarimetry (Antonucci and Miller 1985). The evidence in QSOs for beamed radiation is less direct, but is still suggestive (see Barthel 1989). It seems quite natural, then, to suppose that similar processes occur in the powerful radio galaxies.

This naturally leads us to consider the so-called unified models of active galaxies (Scheuer and Readhead 1979; Blandford and Königl 1979; Orr and Browne 1982; Kapahi and Saikia 1982) and the quasar–radio galaxy unification picture of Barthel (1989) in particular. The rough correspondence between the isotropic ionizing photon flux and that of QSOs in particular suggests that if we saw 3C 294 beam-on, we might well have classified it as a quasar. The differing ionization of the emission lines and radio galaxies poses a problem for this simple picture. As discussed above, a rather steep ($\alpha \sim -1.5$) input spectrum is required to produce the observed He II/C IV ratio. The best-fitting models for QSO emission lines require input spectra with power-law slopes of $\alpha \approx -0.5$ to -0.7. Simply diluting a $\nu^{-0.5}$ spectrum to a low ionization parameter will not reproduce the observed rough equality of C IV λ1550, He II λ1640, C III] λ1909, and C II] λ2326 that are characteristic of the luminous radio galaxies (see Netzer, Elitzur, and Ferland 1985). This suggests that the intrinsic far-UV spectra of the central engines of quasars and radio galaxies differ.

If 3C 294 and other high-luminosity radio galaxies are oriented preferentially in the plane of the sky, there may be dynamical problems in interpreting the emission-line velocities. Barthel (1989) proposes that the mean orientation angle for radio galaxies is 69°. The total amplitudes of the velocity fields of the extended gas will then be a factor of 2 larger. With a typical scale of 60 kpc, this requires masses of the order of 10^{13} $M_\odot$ to keep the gas bound. Such masses are near the upper limit of plausible dynamical masses.

g) Radiative Transfer Effects in the Lyα *Line*

In this section we consider whether optical depth effects could be important in determining the Lyα line profile and velocity field. A number of authors have considered the transfer of Lyα in gaseous nebulae (Adams 1975; Urbaniak and Wolfe 1981; Neufeld and McKee 1988). These authors find that, for large τ, the line profile becomes double-peaked and most of the photons escape through the damping wings. In Figure 6 we show line profiles of Lyα at two locations in the emission-line cloud. The line profile in the lower panel is from the region north of the core and is summed over 2″. The upper panel shows the profile in the region surrounding the southern radio knot. This profile clearly shows excess emission to the blue of line center, relative both to the instrumental profile and

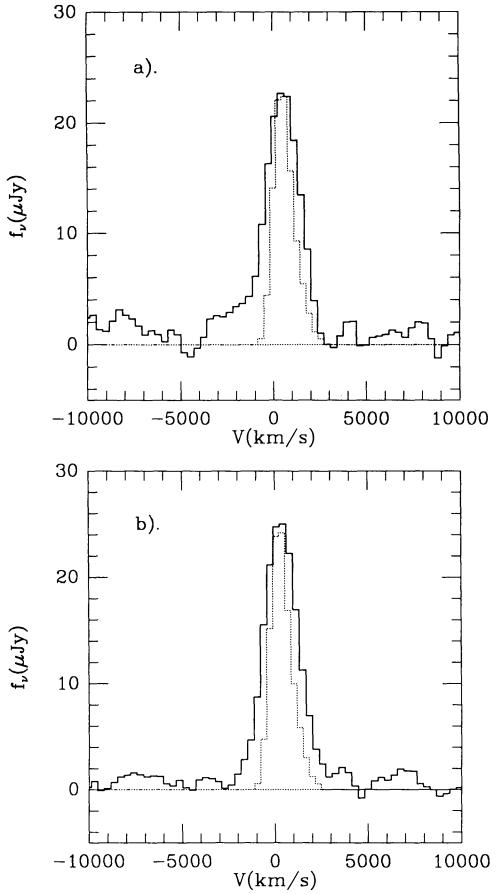

FIG. 6.—Two one-dimensional spectra extractions showing the profile of Lyα. (*a*) Lyα profile in the region north of the radio core ($\delta^* = 39$–41). (*b*) Region centered on the southern radio knot ($\delta^* = 36$–38). This panel shows the blue wing to Lyα quite clearly. In each panel the instrumental profile is shown as a dotted curve.

to the Lyα emission in other regions of the cloud. This line asymmetry is seen independently in five contiguous single-column spectra and in the MMT aperture spectra centered on the southern knot. Thus we are confident that it is not a spurious instrumental feature. This blue wing is not as prominent, in terms of the fraction of the light in the wing relative to the rest of the line, as that in 3C 326.1, as shown in Djorgovski (1988) and Strauss *et al.* (1987). A common explanation for line asymmetries in AGNs requires dust obscuration of the far hemisphere of a symmetric outflow from the central source (Heckman, van Breugel, and Miley 1984; Taniguchi 1987). The *IRAS*-selected galaxies of Armus, Heckman, and Miley (1988), and in particular IRAS 01003−2238 discussed above, show large line widths (~ 1000 km s^{-1}) and large blue wings in the nebular lines. Such an explanation is probably inapplicable in these two cases for a number of reasons. First, it is unlikely that extinction plays a large role in any of the high-redshift radio galaxies, since even rather small amounts of dust effectively squelch the Lyα emission (Hartmann *et al.* 1988). The large line widths of Lyα also argue against a scenario in which resonant scattering with only very small amounts of dust destroy Lyα selectively, since large line widths reduce the number of scatterings required for each Lyα photon to escape the nebulae. Furthermore, in the two cases with the large blue wings, 3C 326.1 and 3C 294, the line asymmetries occur in spatially

resolved regions associated with extranuclear features in the radio source structure, rather than at the location of the nucleus.

A possible explanation in the case of 3C 294 is that the region of blueshifted C IV has corresponding Lyα emission that produces the observed asymmetry. While it is likely that the blueshifted C IV emission south of the core has some Lyα emission associated with it (see Figs. 4*a* and 4*b*), the C IV emission does not extend far enough in the spatial dimension (see Fig. 5) or in the spectral dimension to account for the observed Lyα profile. The blue wing shown in Figure 6 extends to velocities as large as 2500–3500 km s^{-1}. The exact extent is difficult to determine because the signal-to-noise ratio is poorer on the blueward side of Lyα.

A novel explanation for these observations has recently been suggested by Neufeld and McKee (1988). In their model the asymmetry arises as a combination of optical depth effects and multiple scatterings off moving shock fronts in partially ionized regions of the cloud. This "Fermi-acceleration–like" process only applies to lines with very large optical depths, Lyα being (far and away) the best observable line for this. An ideal way to check this model is to examine the line profiles of low optical depth lines. Unfortunately, as Figure 4*b* shows, there is very little C IV or He II emission at the location of the southern knot, and so we were not able to make such a test. Observations of Balmer series lines in the infrared would be the most practical approach.

IV. SUMMARY

We have presented optical, infrared, and radio observations of the powerful radio source 3C 294, which is surrounded by a large cloud of ionized gas. The galaxy is faint in the rest-frame UV, yet has a near-IR luminosity that is typical of radio galaxies at redshifts of order 2. In contrast to the large extent of the ionized gas, the *K*-band image is quite compact.

The emission-line cloud is closely aligned with the radio source axis and has an ionization state indicative of ionization by a nonstellar source. We suggest that the emission-line cloud is photoionized by a central source associated with the galaxy nucleus.

The velocity field of the gas has both large ordered motions and large turbulent components. The total mass required to keep the gas bound to the system is comparable to present-day massive galaxies and their halos. The velocity fields of the high-ionization lines are systematically different from Lyα in a manner that is not easily understood.

This object appears to be one of the most extreme examples of a class of objects characterized by strong and spatially extended Lyα emission associated with a radio source. Other objects of this same class have recently been found at larger redshifts (e.g., 4C 41.17, Chambers, Miley, and van Breugel 1990; M2104−252, McCarthy *et al.* 1990). These objects provide us with a unique opportunity to observe active galaxies in what appears to be a very early stage of their development.

We would like to thank the staffs of the Lick Observatory, the Multiple Mirror Observatory, the Kitt Peak National Observatory, and the National Radio Astronomy Observatory for their expert assistance with the observations. We also thank Robert Laing and Frazer Owen for communicating early radio data, John Huchra for obtaining an observation of 3C 294 with the MMT, and John Stauffer for suggesting the final *J*-band reduction step. Finally, we thank the referee for helpful comments. This research was supported by grants AST 85-13416 (H. S.) and AST 84-16177 (W. vB.) from the National Science Foundation and by the Carnegie Institution of Washington (P. M.), and the California Institute of Technology and Harvard University (S. D.). The Lick Observatory is operated by the University of California and is supported in part by grant AST 86-14510 for the National Science Foundation.

REFERENCES

Adams, T. F. 1975, *Ap. J.*, **201**, 350.
Alexander, P. A., and Leahy, J. P. 1987, *M.N.R.A.S.*, **225**, 1.
Antonucci, R. R. J., and Miller, J. S. 1985, *Ap. J.*, **297**, 621.
Armus, L., Heckman, T. M., and Miley, G. K. 1988, *Ap. J. (Letters)*, **326**, L45.
Barthel, P. D. 1989, *Ap. J.*, **336**, 606.
Baum, S. A., and Heckman, T. M. 1989*a*, *Ap. J.*, **336**, 681.
———. 1989*b*, *Ap. J.*, **336**, 702.
Blandford, R. D., and Königl, A. 1979, *Ap. J.*, **232**, 34.
Chambers, K. C., and McCarthy, P. J. 1990, *Ap. J. (Letters)*, **354**, L9.
Chambers, K. C., Miley, G. K., and van Breugel, W. J. M. 1987, *Nature*, **329**, 604.
———. 1990, *Ap. J.*, **363**, 21.
Crawford, C., Fabian, A. C., Johnstone, R., and Thomas, P. 1988, *M.N.R.A.S.*, **235**, 183.
Danziger, I. J., and Focardi, P. 1988, in *Cooling Flows in Clusters and Galaxies*, ed. A. C. Fabian (Dordrecht: Kluwer), p. 73.
De Young, D. S. 1986, *Ap. J.*, **307**, 62.
di Serego Alighieri, S., Fosbury, R. A. E., Quinn, P. E., and Tadhunter, C. N. 1988, *Nature*, **334**, 591.
Djorgovski, S. 1988, in *Towards Understanding Galaxies at Large Redshifts*, ed. R. G. Kron and A. Renzini (Dordrecht: Kluwer), p. 259.
Eisenhardt, P., and Chokshi, A. 1990, *Ap. J. (Letters)*, **351**, L9.
Elias, J. H., Frogel, J. A., Matthews, K., and Neugebauer, G. 1982, *A.J.*, **87**, 1029.
Fabian, A. C., Arnaud, K. A., Nulsen, P. E., and Mushotzky, R. 1986, *Ap. J.*, **305**, 9.
Fabian, A. C., Crawford, C. S., Johnston, R. M., and Thomas, P. A. 1987, *M.N.R.A.S.*, **228**, 963.
Fabricant, D., and Gorenstein, P. 1983, *Ap. J.*, **267**, 535.
Ferland, G. J. 1981, private communication to H. Spinrad.
Ferland, G. J., and Osterbrock, D. E. 1986, *Ap. J.*, **300**, 658.
Filippenko, A. V. 1985, *Pub. A.S.P.*, **94**, 715.
Fosbury, R. A. E. 1986, in *Structure and Evolution of Active Galactic Nuclei*, ed. G. Giuricin, F. Mardirossian, M. Mezzetti, and M. Ramonella (Dordrecht: Reidel), p. 297.
Garmany, K., and Conti, P. 1982, in *IAU Symposium 99, Wolf-Rayet Stars: Observations, Physics, Evolution*, ed. C. W. H. de Loore and A. J. Willis (Dordrecht: Reidel), p. 106.
Gopal-Krishna, G.-K., and Wiita, P. J. 1987, *M.N.R.A.S.*, **226**, 531.
Hamilton, D. 1985, *Ap. J.*, **297**, 371.
Hartigan, P., Raymond, J., and Hartmann, L. 1987, *Ap. J.*, **316**, 323.
Hartmann, L. W., Huchra, J. P., Geller, M. J., O'Brien, P., and Wilson, R. 1988, *Ap. J.*, **326**, 101.
Heckman, T. M., Baum, S. A., van Breugel, W. J. M., and McCarthy, P. J. 1989, *Ap. J.*, **338**, 48.
Heckman, T. M., van Breugel, W. J. M., and Miley, G. K. 1984, *Ap. J.*, **286**, 509.
Hintzen, P., and Stocke, J. T. 1986, *Ap. J.*, **308**, 540.
Hu, E. M. 1988, in *Cooling Flows in Clusters and Galaxies*, ed. A. C. Fabian, (Dordrecht: Kluwer), p. 73.
Hu, E. M., Cowie, L. L., and Wang, Z. 1985, *Ap. J. Suppl.*, **59**, 447.
Jenkins, C. J., Pooley, G. G., and Riley, J. M. 1977, *Mem. R.A.S.*, **84**, 61.
Kapahi, V. K., and Saikia, D. K. 1982, *J. Ap. Astr.*, **3**, 465.
Kellermann, K. I., Pauliny-Toth, I. I. K., and Williams, P. J. S. 1969, *Ap. J.*, **157**, 1.
Kennicutt, R. 1983, *Ap. J.*, **272**, 54.
Kristian, J., Sandage, A., and Katem, B. 1974, *Ap. J.*, **191**, 43.
Latham, D. 1982, in *IAU Colloquium 67, Instrumentation for Astronomy with Large Optical Telescopes*, ed. C. Humphries (Dordrecht: Reidel), p. 259.
Lilly, S. J. 1988, *Ap. J.*, **333**, 161.
———. 1989, *Ap. J.*, **340**, 77.
McCarthy, P. J., Kapahi, V. K., van Breugel, W. J. M., and Subrahmanya, C. R. 1990, *A.J.*, in press.
McCarthy, P. J., Spinrad, H., Djorgovski, S. G., Strauss, M. A., van Breugel, M. J. M., and Liebert, J. 1987*a*, *Ap. J. (Letters)*, **319**, L39.

McCarthy, P. J., Spinrad, H., van Breugel, W. J. M., Djorgovski, S., Strauss, M. A., and Dickinson, M. 1988, in *Cooling Flows in Clusters and Galaxies*, ed. A. C. Fabian (Dordrecht: Kluwer), p. 325.
McCarthy, P. J., and van Breugel, W. J. M. 1989, in *The Epoch of Galaxy Formation*, ed. C. Frenk, R. Ellis, T. Shanks, A. Heavens, and J. Peacock (Dordrecht: Kluwer), p. 57.
McCarthy, P. J., van Breugel, W. J. M., and Kapahi, V. K. 1990, *Ap. J.*, in press.
McCarthy, P. J., van Breugel, W. J. M., Spinrad, H., and Djorgovski, S. G. 1987*b*, *Ap. J. (Letters)*, **321**, L29.
Miley, G. K. 1983, *Ann. Rev. Astr. Ap.*, **18**, 165.
Miller, J. S., and Stone, R. P. S. 1988, *The Lick* 3 m *Cassegrain CCD Spectrograph* (*Lick Obs. Tech. Bull.*, No. 48).
Myers, S. T., and Spangler, S. R. 1985, *Ap. J.*, **291**, 52.
Netzer, H., Elitzur, M., and Ferland, G. J. 1985, *Ap. J.*, **299**, 752.
Neufeld, D. A., and McKee, C. F. 1988, *Ap. J. (Letters)*, **331**, L87.
Neugebauer, G., Oke, J. B., Becklin, E. E., and Mathews, K. 1979, *Ap. J.*, **230**, 79.
Norgaard-Nielsen, H. U., Jorgensen, H. E., and Hansen, L. 1984, *Astr. Ap.*, **135**, L3.
Oke, J. B. 1974, *Ap. J.*, **188**, 443.
Orr, M. J. L., and Browne, I. W. A. 1982, *M.N.R.A.S.*, **200**, 1067.
Osterbrock, D. E., and Cohen, R. D. 1982, *Ap. J.*, **261**, 64.
Pedelty, J. A., Rudnick, L., McCarthy, P. J., and Spinrad, H. 1989*a*, *A.J.*, **97**, 647.
———. 1989*b*, *A.J.*, **98**, 1232.
Pogge, R. W. 1988, *Ap. J.*, **328**, 519.
Probst, R. G. 1988, Infrared Array User Manual (NOAO internal publication).
Riley, J. M., Longair, M. S., and Gunn, J. E. 1980, *M.N.R.A.S.*, **192**, 233.
Robinson, A., Binetta, L., Fosbury, R. A. E., and Tadhunter, C. N. 1987, *M.N.R.A.S.*, **227**, 97.
Scarrott, S. M., Rolph, C. D., and Tadhunter, C. N. 1990, *M.N.R.A.S.*, **243**, 5P.
Scheuer, P. A. G., and Readhead, A. C. S. 1979, *Nature*, **277**, 182.
Shull, J. M., and McKee, C. F. 1979, *Ap. J.*, **227**, 131.
Spinrad, H. 1987, in *High Redshift and Primeval Galaxies*, ed. J. Bergeron, D. Kunth, B. Rocca-Volmerange, and J. Tran Thanh Van (Gif-sur-Yvette: Editions Frontières), p. 59.
Spinrad, H., and Djorgovski, S. 1984*a*, *Ap. J. (Letters)*, **280**, L9.
———. 1984*b*, *Ap. J. (Letters)*, **285**, L49.
Spinrad, H., Filippenko, A. V., Wyckoff, S., Stocke, J. T., Wagner, R. M., and Lawrie, D. G. 1985, *Ap. J. (Letters)*, **299**, L7.
Stasinska, G. 1984, *Astr. Ap. Suppl.*, **48**, 299.
Stone, R. P. S. 1977, *Ap. J.*, **218**, 767.
Strauss, M. A., McCarthy, P. J., Spinrad, H., Djorgovski, S., van Breugel, W. J. M., and Liebert, J. 1987, in *High Redshift and Primeval Galaxies*, ed. J. Bergeron, D. Kunth, B. Rocca-Volmerange, and J. Tran Thanh Van (Gif-sur-Yvette: Editions Frontières), p. 85.
Tadhunter, C. N., and Tsvetanov, Z. 1989, *Nature*, **341**, 422.
Taniguchi, Y. 1987, *Ap. J. (Letters)*, **317**, L57.
Terlevich, R., and Melnick, J. 1985, *M.N.R.A.S.*, **213**, 813.
Thompson, A. R., Clark, B. G., Wade, C. M., and Napier, P. J. 1980, *Ap. J. Suppl.*, **44**, 151.
Urbaniak, J. J., and Wolfe, A. M. 1981, *Ap. J.*, **244**, 406.
van Breugel, W. J. M. 1986, in *Proc. Toronto Conf. on Jets from Stars and Galaxies*, ed. R. N. Henriksen and T. W. Jones (*Canadian J. Physi.*, Vol. **64**), p. 392.
van Breugel, W. J. M., Heckman, T. M., Miley, G. K., and Filippenko, A. V. 1986, *Ap. J.*, **311**, 58.
Véron, P. 1966, *Ap. J.*, **144**, 861.
Wilson, A. S., Ward, M. J., and Haniff, C. A. 1988, *Ap. J.*, **334**, 121.

MARK DICKINSON, WIL VAN BREUGEL, and HYRON SPINRAD: Astronomy Department, 601 Campbell Hall, University of California, Berkeley, CA 94720

S. DJORGOVSKI: Astronomy, 10–24, Robinson Hall, California Institute of Technology, Pasadena, CA 91101

PETER EISENHARDT: MS 245-6, NASA–Ames Research Center, Moffett Field, CA 94035

JAMES LIEBERT: Steward Observatory, University of Arizona, Tucson, AZ 85720

PATRICK J. MCCARTHY: The Observatories of the Carnegie Institution of Washington, 813 Santa Barbara Street, Pasadena, CA 91101